Research Article | Vol. 25, No. 4 | 20 Feb 2017 | OPTICS EXPRESS 3196

Optics EXPRESS

Determination of the refractive index and thickness of a hydroxide-catalysis bond between fused silica from reflectivity measurements

V. Mangano,[1] A. A. van Veggel,[1,*] R. Douglas,[1] J. Faller,[2] A. Grant,[1] J. Hough,[1] and S. Rowan[1]

[1]*SUPA, School of Physics and Astronomy, University of Glasgow, Glasgow G12 8QQ, Scotland, UK*
[2]*JILA, University of Colorado, 440 UCB, Boulder, CO 80309, USA*
[*]*Marielle.vanVeggel@glasgow.ac.uk*

Abstract: Hydroxide-catalysis bonding is a high precision jointing technique producing strong, transparent and thin bonds, the use of which in the delicate fused silica mirror suspensions of aLIGO have been instrumental in the first detections of gravitational radiation. More sensitive future gravitational wave detectors will require more accurate (ideally in situ) measurements of properties such as bond thickness. Here a non-destructive technique is presented in which the thickness and refractive index of a bond are determined from measurements of optical reflectivity. The reflectivity of a bond made between two fused silica discs using sodium silicate solution is less than $1{\cdot}10^{-3}$ after 3 months. The thickness decreases to a constant value of around 140 nm at its minimum and the refractive index increases from 1.36 to 1.45. This proves that as well as determination of bond thickness in situ this bonding technique is highly interesting for optical applications.

OCIS codes: (000.2170) Equipment and techniques; (120.5700) Reflection; (160.6030) Silica; (160.4760) Optical properties; (310.6870) Thin films, other properties.

References and links

1. T. S. Rutherford, "An edge-pumped YB:YAG slab laser and phased array resonator," Ph.D. Thesis, Stanford University (2001).
2. A. Taylor, L. d'Arcio, J. Bogenstahl, K. Danzmann, C. Diekmann, E. D. Fitzsimons, O. Gerberding, G. Heinzel, J.-S. Hennig, H. Hogenhuis, C. J. Killow, M. Lieser, S. Lucarelli, S. Nikolov, M. Perreur-Lloyd, J. Pijnenburg, D. I. Robertson, A. Sohmer, M. Tröbs, H. Ward, and D. Weise, "Optical Bench Interferometer - From LISA Pathfinder to NGO/eLISA," in *Proceedings of ASP Conference Series on the 9th LISA Symposium*, G. Auger, P. Binétruy, and E. Plagnol, eds. (Astronomical Society of the Pacific, 2013), pp. 311–315.
3. L. Cunningham, P. G. Murray, A. Cumming, E. J. Elliffe, G. D. Hammond, K. Haughian, J. Hough, M. Hendry, R. Jones, I. W. Martin, S. Reid, S. Rowan, J. Scott, K. A. Strain, K. Tokmakov, C. Torrie, and A. A. van Veggel, "Re-evaluation of the mechanical loss factor of hydroxide-catalysis bonds and its significance for the next generation of gravitational wave detectors," Phys. Lett. A **374**(39), 3993–3998 (2010).
4. A. A. van Veggel and C. J. Killow, "Hydroxide catalysis bonding for astronomical instruments," Adv. Opt. Technol. **3**(3), 293–307 (2014).
5. A. V. Cumming, A. S. Bell, L. Barsotti, M. A. Barton, G. Cagnoli, D. Cook, L. Cunningham, M. Evans, G. D. Hammond, G. M. Harry, A. Heptonstall, J. Hough, R. Jones, R. Kumar, R. Mittleman, N. A. Robertson, S. Rowan, B. Shapiro, K. A. Strain, K. Tokmakov, C. Torrie, and A. A. van Veggel, "Design and development of the advanced LIGO monolithic fused silica suspension," Class. Quantum Gravity **29**(3), 035003 (2012).
6. B. P. Abbott, R. Abbott, T. D. Abbott, M. R. Abernathy, F. Acernese, K. Ackley, C. Adams, T. Adams, P. Addesso, R. X. Adhikari, V. B. Adya, C. Affeldt, M. Agathos, K. Agatsuma, N. Aggarwal, O. D. Aguiar, L. Aiello, A. Ain, P. Ajith, B. Allen, A. Allocca, P. A. Altin, S. B. Anderson, W. G. Anderson, K. Arai, M. A. Arain, M. C. Araya, C. C. Arceneaux, J. S. Areeda, N. Arnaud, K. G. Arun, S. Ascenzi, G. Ashton, M. Ast, S. M. Aston, P. Astone, P. Aufmuth, C. Aulbert, S. Babak, P. Bacon, M. K. Bader, P. T. Baker, F. Baldaccini, G. Ballardin, S. W. Ballmer, J. C. Barayoga, S. E. Barclay, B. C. Barish, D. Barker, F. Barone, B. Barr, L. Barsotti, M. Barsuglia, D. Barta, J. Bartlett, M. A. Barton, I. Bartos, R. Bassiri, A. Basti, J. C. Batch, C. Baune, V. Bavigadda, M. Bazzan, B. Behnke, M. Bejger, C. Belczynski, A. S. Bell, C. J. Bell, B. K. Berger, J. Bergman, G. Bergmann, C. P. Berry, D. Bersanetti, A. Bertolini, J. Betzwieser, S. Bhagwat, R. Bhandare, I. A. Bilenko, G. Billingsley, J. Birch, R. Birney, O. Birnholtz, S. Biscans, A. Bisht, M. Bitossi, C. Biwer, M. A. Bizouard, J. K. Blackburn, C. D. Blair, D. G. Blair, R. M. Blair, S. Bloemen, O. Bock, T. P. Bodiya, M. Boer, G. Bogaert, C. Bogan, A. Bohe, P. Bojtos, C. Bond, F. Bondu, R. Bonnand, B. A. Boom, R. Bork, V. Boschi, S. Bose, Y. Bouffanais, A. Bozzi, C. Bradaschia, P. R. Brady, V. B. Braginsky, M. Branchesi, J. E. Brau, T. Briant, A.

#278772 https://doi.org/10.1364/OE.25.003196
Journal © 2017 Received 2 Nov 2016; revised 23 Dec 2016; accepted 23 Dec 2016; published 7 Feb 2017

Optics EXPRESS

Brillet, M. Brinkmann, V. Brisson, P. Brockill, A. F. Brooks, D. A. Brown, D. D. Brown, N. M. Brown, C. C. Buchanan, A. Buikema, T. Bulik, H. J. Bulten, A. Buonanno, D. Buskulic, C. Buy, R. L. Byer, M. Cabero, L. Cadonati, G. Cagnoli, C. Cahillane, J. Calderón Bustillo, T. Callister, E. Calloni, J. B. Camp, K. C. Cannon, J. Cao, C. D. Capano, E. Capocasa, F. Carbognani, S. Caride, J. Casanueva Diaz, C. Casentini, S. Caudill, M. Cavaglià, F. Cavalier, R. Cavalieri, G. Cella, C. B. Cepeda, L. Cerboni Baiardi, G. Cerretani, E. Cesarini, R. Chakraborty, T. Chalermsongsak, S. J. Chamberlin, M. Chan, S. Chao, P. Charlton, E. Chassande-Mottin, H. Y. Chen, Y. Chen, C. Cheng, A. Chincarini, A. Chiummo, H. S. Cho, M. Cho, J. H. Chow, N. Christensen, Q. Chu, S. Chua, S. Chung, G. Ciani, F. Clara, J. A. Clark, F. Cleva, E. Coccia, P. F. Cohadon, A. Colla, C. G. Collette, L. Cominsky, M. Constancio, Jr., A. Conte, L. Conti, D. Cook, T. R. Corbitt, N. Cornish, A. Corsi, S. Cortese, C. A. Costa, M. W. Coughlin, S. B. Coughlin, J. P. Coulon, S. T. Countryman, P. Couvares, E. E. Cowan, D. M. Coward, M. J. Cowart, D. C. Coyne, R. Coyne, K. Craig, J. D. Creighton, T. D. Creighton, J. Cripe, S. G. Crowder, A. M. Cruise, A. Cumming, L. Cunningham, E. Cuoco, T. Dal Canton, S. L. Danilishin, S. D'Antonio, K. Danzmann, N. S. Darman, C. F. Da Silva Costa, V. Dattilo, I. Dave, H. P. Daveloza, M. Davier, G. S. Davies, E. J. Daw, R. Day, S. De, D. DeBra, G. Debreczeni, J. Degallaix, M. De Laurentis, S. Deléglise, W. Del Pozzo, T. Denker, T. Dent, H. Dereli, V. Dergachev, R. T. DeRosa, R. De Rosa, R. DeSalvo, S. Dhurandhar, M. C. Díaz, L. Di Fiore, M. Di Giovanni, A. Di Lieto, S. Di Pace, I. Di Palma, A. Di Virgilio, G. Dojcinoski, V. Dolique, F. Donovan, K. L. Dooley, S. Doravari, R. Douglas, T. P. Downes, M. Drago, R. W. Drever, J. C. Driggers, Z. Du, M. Ducrot, S. E. Dwyer, T. B. Edo, M. C. Edwards, A. Effler, H. B. Eggenstein, P. Ehrens, J. Eichholz, S. S. Eikenberry, W. Engels, R. C. Essick, T. Etzel, M. Evans, T. M. Evans, R. Everett, M. Factourovich, V. Fafone, H. Fair, S. Fairhurst, X. Fan, Q. Fang, S. Farinon, B. Farr, W. M. Farr, M. Favata, M. Fays, H. Fehrmann, M. M. Fejer, D. Feldbaum, I. Ferrante, E. C. Ferreira, F. Ferrini, F. Fidecaro, L. S. Finn, I. Fiori, D. Fiorucci, R. P. Fisher, R. Flaminio, M. Fletcher, H. Fong, J. D. Fournier, S. Franco, S. Frasca, F. Frasconi, M. Frede, Z. Frei, A. Freise, R. Frey, V. Frey, T. T. Fricke, P. Fritschel, V. V. Frolov, P. Fulda, M. Fyffe, H. A. Gabbard, J. R. Gair, L. Gammaitoni, S. G. Gaonkar, F. Garufi, A. Gatto, G. Gaur, N. Gehrels, G. Gemme, B. Gendre, E. Genin, A. Gennai, J. George, L. Gergely, V. Germain, A. Ghosh, A. Ghosh, S. Ghosh, J. A. Giaime, K. D. Giardina, A. Giazotto, K. Gill, A. Glaefke, J. R. Gleason, E. Goetz, R. Goetz, L. Gondan, G. González, J. M. Gonzalez Castro, A. Gopakumar, N. A. Gordon, M. L. Gorodetsky, S. E. Gossan, M. Gosselin, R. Gouaty, C. Graef, P. B. Graff, M. Granata, A. Grant, S. Gras, C. Gray, G. Greco, A. C. Green, R. J. Greenhalgh, P. Groot, H. Grote, S. Grunewald, G. M. Guidi, X. Guo, A. Gupta, M. K. Gupta, K. E. Gushwa, E. K. Gustafson, R. Gustafson, J. J. Hacker, B. R. Hall, E. D. Hall, G. Hammond, M. Haney, M. M. Hanke, J. Hanks, C. Hanna, M. D. Hannam, J. Hanson, T. Hardwick, J. Harms, G. M. Harry, I. W. Harry, M. J. Hart, M. T. Hartman, C. J. Haster, K. Haughian, J. Healy, J. Heefner, A. Heidmann, M. C. Heintze, G. Heinzel, H. Heitmann, P. Hello, G. Hemming, M. Hendry, I. S. Heng, J. Hennig, A. W. Heptonstall, M. Heurs, S. Hild, D. Hoak, K. A. Hodge, D. Hofman, S. E. Hollitt, K. Holt, D. E. Holz, P. Hopkins, D. J. Hosken, J. Hough, E. A. Houston, E. J. Howell, Y. M. Hu, S. Huang, E. A. Huerta, D. Huet, B. Hughey, S. Husa, S. H. Huttner, T. Huynh-Dinh, A. Idrisy, N. Indik, D. R. Ingram, R. Inta, H. N. Isa, J. M. Isac, M. Isi, G. Islas, T. Isogai, B. R. Iyer, K. Izumi, M. B. Jacobson, T. Jacqmin, H. Jang, K. Jani, P. Jaranowski, S. Jawahar, F. Jiménez-Forteza, W. W. Johnson, N. K. Johnson-McDaniel, D. I. Jones, R. Jones, R. J. Jonker, L. Ju, K. Haris, C. V. Kalaghatgi, V. Kalogera, S. Kandhasamy, G. Kang, J. B. Kanner, S. Karki, M. Kasprzack, E. Katsavounidis, W. Katzman, S. Kaufer, T. Kaur, K. Kawabe, F. Kawazoe, F. Kéfélian, M. S. Kehl, D. Keitel, D. B. Kelley, W. Kells, R. Kennedy, D. G. Keppel, J. S. Key, A. Khalaidovski, F. Y. Khalili, I. Khan, S. Khan, Z. Khan, E. A. Khazanov, N. Kijbunchoo, C. Kim, J. Kim, K. Kim, N. G. Kim, N. Kim, Y. M. Kim, E. J. King, P. J. King, D. L. Kinzel, J. S. Kissel, L. Kleybolte, S. Klimenko, S. M. Koehlenbeck, K. Kokeyama, S. Koley, V. Kondrashov, A. Kontos, S. Koranda, M. Korobko, W. Z. Korth, I. Kowalska, D. B. Kozak, V. Kringel, B. Krishnan, A. Królak, C. Krueger, G. Kuehn, P. Kumar, R. Kumar, L. Kuo, A. Kutynia, P. Kwee, B. D. Lackey, M. Landry, J. Lange, B. Lantz, P. D. Lasky, A. Lazzarini, C. Lazzaro, P. Leaci, S. Leavey, E. O. Lebigot, C. H. Lee, H. K. Lee, H. M. Lee, K. Lee, A. Lenon, M. Leonardi, J. R. Leong, N. Leroy, N. Letendre, Y. Levin, B. M. Levine, T. G. Li, A. Libson, T. B. Littenberg, N. A. Lockerbie, J. Logue, A. L. Lombardi, L. T. London, J. E. Lord, M. Lorenzini, V. Loriette, M. Lormand, G. Losurdo, J. D. Lough, C. O. Lousto, G. Lovelace, H. Lück, A. P. Lundgren, J. Luo, R. Lynch, Y. Ma, T. MacDonald, B. Machenschalk, M. MacInnis, D. M. Macleod, F. Magaña-Sandoval, R. M. Magee, M. Mageswaran, E. Majorana, I. Maksimovic, V. Malvezzi, N. Man, I. Mandel, V. Mandic, V. Mangano, G. L. Mansell, M. Manske, M. Mantovani, F. Marchesoni, F. Marion, S. Márka, Z. Márka, A. S. Markosyan, E. Maros, F. Martelli, L. Martellini, I. W. Martin, R. M. Martin, D. V. Martynov, J. N. Marx, K. Mason, A. Masserot, T. J. Massinger, M. Masso-Reid, F. Matichard, L. Matone, N. Mavalvala, N. Mazumder, G. Mazzolo, R. McCarthy, D. E. McClelland, S. McCormick, S. C. McGuire, G. McIntyre, J. McIver, D. J. McManus, S. T. McWilliams, D. Meacher, G. D. Meadors, J. Meidam, A. Melatos, G. Mendell, D. Mendoza-Gandara, R. A. Mercer, E. Merilh, M. Merzougui, S. Meshkov, C. Messenger, C. Messick, P. M. Meyers, F. Mezzani, H. Miao, C. Michel, H. Middleton, E. E. Mikhailov, L. Milano, J. Miller, M. Millhouse, Y. Minenkov, J. Ming, S. Mirshekari, C. Mishra, S. Mitra, V. P. Mitrofanov, G. Mitselmakher, R. Mittleman, A. Moggi, M. Mohan, S. R. Mohapatra, M. Montani, B. C. Moore, C. J. Moore, D. Moraru, G. Moreno, S. R. Morriss, K. Mossavi, B. Mours, C. M. Mow-Lowry, C. L. Mueller, G. Mueller, A. W. Muir, A. Mukherjee, D. Mukherjee, S. Mukherjee, N. Mukund, A. Mullavey, J. Munch, D. J. Murphy, P. G. Murray, A. Mytidis, I. Nardecchia, L. Naticchioni, R. K. Nayak, V. Necula, K. Nedkova, G. Nelemans, M. Neri, A. Neunzert, G. Newton, T. T. Nguyen, A. B. Nielsen, S. Nissanke, A. Nitz, F. Nocera, D. Nolting, M. E. Normandin, L. K. Nuttall, J. Oberling, E. Ochsner, J. O'Dell, E. Oelker, G. H. Ogin, J. J. Oh, S. H. Oh, F. Ohme, M. Oliver, P. Oppermann, R. J. Oram, B. O'Reilly, R. O'Shaughnessy, C. D. Ott, D. J. Ottaway, R. S. Ottens, H. Overmier, B. J. Owen, A. Pai, S. A. Pai, J. R. Palamos, O. Palashov, C. Palomba, A. Pal-Singh, H. Pan, Y. Pan, C. Pankow, F. Pannarale, B. C. Pant, F. Paoletti, A. Paoli, M. A. Papa, H. R. Paris, W. Parker, D. Pascucci, A. Pasqualetti, R. Passaquieti, D.

Optics EXPRESS

Passuello, B. Patricelli, Z. Patrick, B. L. Pearlstone, M. Pedraza, R. Pedurand, L. Pekowsky, A. Pele, S. Penn, A. Perreca, H. P. Pfeiffer, M. Phelps, O. Piccinni, M. Pichot, M. Pickenpack, F. Piergiovanni, V. Pierro, G. Pillant, L. Pinard, I. M. Pinto, M. Pitkin, J. H. Poeld, R. Poggiani, P. Popolizio, A. Post, J. Powell, J. Prasad, V. Predoi, S. S. Premachandra, T. Prestegard, L. R. Price, M. Prijatelj, M. Principe, S. Privitera, R. Prix, G. A. Prodi, L. Prokhorov, O. Puncken, M. Punturo, P. Puppo, M. Pürrer, H. Qi, J. Qin, V. Quetschke, E. A. Quintero, R. Quitzow-James, F. J. Raab, D. S. Rabeling, H. Radkins, P. Raffai, S. Raja, M. Rakhmanov, C. R. Ramet, P. Rapagnani, V. Raymond, M. Razzano, V. Re, J. Read, C. M. Reed, T. Regimbau, L. Rei, S. Reid, D. H. Reitze, H. Rew, S. D. Reyes, F. Ricci, K. Riles, N. A. Robertson, R. Robie, F. Robinet, A. Rocchi, L. Rolland, J. G. Rollins, V. J. Roma, J. D. Romano, R. Romano, G. Romanov, J. H. Romie, D. Rosińska, S. Rowan, A. Rüdiger, P. Ruggi, K. Ryan, S. Sachdev, T. Sadecki, L. Sadeghian, L. Salconi, M. Saleem, F. Salemi, A. Samajdar, L. Sammut, L. M. Sampson, E. J. Sanchez, V. Sandberg, B. Sandeen, G. H. Sanders, J. R. Sanders, B. Sassolas, B. S. Sathyaprakash, P. R. Saulson, O. Sauter, R. L. Savage, A. Sawadsky, P. Schale, R. Schilling, J. Schmidt, P. Schmidt, R. Schnabel, R. M. Schofield, A. Schönbeck, E. Schreiber, D. Schuette, B. F. Schutz, J. Scott, S. M. Scott, D. Sellers, A. S. Sengupta, D. Sentenac, V. Sequino, A. Sergeev, G. Serna, Y. Setyawati, A. Sevigny, D. A. Shaddock, T. Shaffer, S. Shah, M. S. Shahriar, M. Shaltev, Z. Shao, B. Shapiro, P. Shawhan, A. Sheperd, D. H. Shoemaker, D. M. Shoemaker, K. Siellez, X. Siemens, D. Sigg, A. D. Silva, D. Simakov, A. Singer, L. P. Singer, A. Singh, R. Singh, A. Singhal, A. M. Sintes, B. J. Slagmolen, J. R. Smith, M. R. Smith, N. D. Smith, R. J. Smith, E. J. Son, B. Sorazu, F. Sorrentino, T. Souradeep, A. K. Srivastava, A. Staley, M. Steinke, J. Steinlechner, S. Steinlechner, D. Steinmeyer, B. C. Stephens, S. P. Stevenson, R. Stone, K. A. Strain, N. Straniero, G. Stratta, N. A. Strauss, S. Strigin, R. Sturani, A. L. Stuver, T. Z. Summerscales, L. Sun, P. J. Sutton, B. L. Swinkels, M. J. Szczepańczyk, M. Tacca, D. Talukder, D. B. Tanner, M. Tápai, S. P. Tarabrin, A. Taracchini, R. Taylor, T. Theeg, M. P. Thirugnanasambandam, E. G. Thomas, M. Thomas, P. Thomas, K. A. Thorne, K. S. Thorne, E. Thrane, S. Tiwari, V. Tiwari, K. V. Tokmakov, C. Tomlinson, M. Tonelli, C. V. Torres, C. I. Torrie, D. Töyrä, F. Travasso, G. Traylor, D. Trifirò, M. C. Tringali, L. Trozzo, M. Tse, M. Turconi, D. Tuyenbayev, D. Ugolini, C. S. Unnikrishnan, A. L. Urban, S. A. Usman, H. Vahlbruch, G. Vajente, G. Valdes, M. Vallisneri, N. van Bakel, M. van Beuzekom, J. F. van den Brand, C. Van Den Broeck, D. C. Vander-Hyde, L. van der Schaaf, J. V. van Heijningen, A. A. van Veggel, M. Vardaro, S. Vass, M. Vasúth, R. Vaulin, A. Vecchio, G. Vedovato, J. Veitch, P. J. Veitch, K. Venkateswara, D. Verkindt, F. Vetrano, A. Viceré, S. Vinciguerra, D. J. Vine, J. Y. Vinet, S. Vitale, T. Vo, H. Vocca, C. Vorvick, D. Voss, W. D. Vousden, S. P. Vyatchanin, A. R. Wade, L. E. Wade, M. Wade, S. J. Waldman, M. Walker, L. Wallace, S. Walsh, G. Wang, H. Wang, M. Wang, X. Wang, Y. Wang, H. Ward, R. L. Ward, J. Warner, M. Was, B. Weaver, L. W. Wei, M. Weinert, A. J. Weinstein, R. Weiss, T. Welborn, L. Wen, P. Weßels, T. Westphal, K. Wette, J. T. Whelan, S. E. Whitcomb, D. J. White, B. F. Whiting, K. Wiesner, C. Wilkinson, P. A. Willems, L. Williams, R. D. Williams, A. R. Williamson, J. L. Willis, B. Willke, M. H. Wimmer, L. Winkelmann, W. Winkler, C. C. Wipf, A. G. Wiseman, H. Wittel, G. Woan, J. Worden, J. L. Wright, G. Wu, J. Yablon, I. Yakushin, W. Yam, H. Yamamoto, C. C. Yancey, M. J. Yap, H. Yu, M. Yvert, A. Zadrożny, L. Zangrando, M. Zanolin, J. P. Zendri, M. Zevin, F. Zhang, L. Zhang, M. Zhang, Y. Zhang, C. Zhao, M. Zhou, Z. Zhou, X. J. Zhu, M. E. Zucker, S. E. Zuraw, and J. Zweizig; LIGO Scientific Collaboration and Virgo Collaboration, "Observation of gravitational waves from a binary black hole merger," Phys. Rev. Lett. **116**(6), 061102 (2016).

7. B. P. Abbott, R. Abbott, T. D. Abbott, M. R. Abernathy, F. Acernese, K. Ackley, C. Adams, T. Adams, P. Addesso, R. X. Adhikari, V. B. Adya, C. Affeldt, M. Agathos, K. Agatsuma, N. Aggarwal, O. D. Aguiar, L. Aiello, A. Ain, P. Ajith, B. Allen, A. Allocca, P. A. Altin, S. B. Anderson, W. G. Anderson, K. Arai, M. C. Araya, C. C. Arceneaux, J. S. Areeda, N. Arnaud, K. G. Arun, S. Ascenzi, G. Ashton, M. Ast, S. M. Aston, P. Astone, P. Aufmuth, C. Aulbert, S. Babak, P. Bacon, M. K. Bader, P. T. Baker, F. Baldaccini, G. Ballardin, S. W. Ballmer, J. C. Barayoga, S. E. Barclay, B. C. Barish, D. Barker, F. Barone, B. Barr, L. Barsotti, M. Barsuglia, D. Barta, J. Bartlett, I. Bartos, R. Bassiri, A. Basti, J. C. Batch, C. Baune, V. Bavigadda, M. Bazzan, M. Bejger, A. S. Bell, B. K. Berger, G. Bergmann, C. P. Berry, D. Bersanetti, A. Bertolini, J. Betzwieser, S. Bhagwat, R. Bhandare, I. A. Bilenko, G. Billingsley, J. Birch, R. Birney, O. Birnholtz, S. Biscans, A. Bisht, M. Bitossi, C. Biwer, M. A. Bizouard, J. K. Blackburn, C. D. Blair, D. G. Blair, R. M. Blair, S. Bloemen, O. Bock, M. Boer, G. Bogaert, C. Bogan, A. Bohe, C. Bond, F. Bondu, R. Bonnand, B. A. Boom, R. Bork, V. Boschi, S. Bose, Y. Bouffanais, A. Bozzi, C. Bradaschia, P. R. Brady, V. B. Braginsky, M. Branchesi, J. E. Brau, T. Briant, A. Brillet, M. Brinkmann, V. Brisson, P. Brockill, J. E. Broida, A. F. Brooks, D. A. Brown, D. D. Brown, N. M. Brown, S. Brunett, C. C. Buchanan, A. Buikema, T. Bulik, H. J. Bulten, A. Buonanno, D. Buskulic, C. Buy, R. L. Byer, M. Cabero, L. Cadonati, G. Cagnoli, C. Cahillane, J. Calderón Bustillo, T. Callister, E. Calloni, J. B. Camp, K. C. Cannon, J. Cao, C. D. Capano, E. Capocasa, F. Carbognani, S. Caride, J. Casanueva Diaz, C. Casentini, S. Caudill, M. Cavaglià, F. Cavalier, R. Cavalieri, G. Cella, C. B. Cepeda, L. Cerboni Baiardi, G. Cerretani, E. Cesarini, S. J. Chamberlin, M. Chan, S. Chao, P. Charlton, E. Chassande-Mottin, B. D. Cheeseboro, H. Y. Chen, Y. Chen, C. Cheng, A. Chincarini, A. Chiummo, H. S. Cho, M. Cho, J. H. Chow, N. Christensen, Q. Chu, S. Chua, S. Chung, G. Ciani, F. Clara, J. A. Clark, F. Cleva, E. Coccia, P. F. Cohadon, A. Colla, C. G. Collette, L. Cominsky, M. Constancio, A. Conte, L. Conti, D. Cook, T. R. Corbitt, N. Cornish, A. Corsi, S. Cortese, C. A. Costa, M. W. Coughlin, S. B. Coughlin, J. P. Coulon, S. T. Countryman, P. Couvares, E. E. Cowan, D. M. Coward, M. J. Cowart, D. C. Coyne, R. Coyne, K. Craig, J. D. Creighton, J. Cripe, S. G. Crowder, A. Cumming, L. Cunningham, E. Cuoco, T. Dal Canton, S. L. Danilishin, S. D'Antonio, K. Danzmann, N. S. Darman, A. Dasgupta, C. F. Da Silva Costa, V. Dattilo, I. Dave, M. Davier, G. S. Davies, E. J. Daw, R. Day, S. De, D. DeBra, G. Debreczeni, J. Degallaix, M. De Laurentis, S. Deléglise, W. Del Pozzo, T. Denker, T. Dent, V. Dergachev, R. De Rosa, R. T. DeRosa, R. DeSalvo, R. C. Devine, S. Dhurandhar, M. C. Díaz, L. Di Fiore, M. Di Giovanni, T. Di Girolamo, A. Di Lieto, S. Di Pace, I. Di Palma, A. Di Virgilio, V. Dolique, F. Donovan, K. L. Dooley, S. Doravari, R. Douglas, T. P. Downes, M. Drago, R. W. Drever, J. C. Driggers, M. Ducrot, S. E.

Optics EXPRESS

Dwyer, T. B. Edo, M. C. Edwards, A. Effler, H. B. Eggenstein, P. Ehrens, J. Eichholz, S. S. Eikenberry, W. Engels, R. C. Essick, T. Etzel, M. Evans, T. M. Evans, R. Everett, M. Factourovich, V. Fafone, H. Fair, S. Fairhurst, X. Fan, Q. Fang, S. Farinon, B. Farr, W. M. Farr, M. Favata, M. Fays, H. Fehrmann, M. M. Fejer, E. Fenyvesi, I. Ferrante, E. C. Ferreira, F. Ferrini, F. Fidecaro, I. Fiori, D. Fiorucci, R. P. Fisher, R. Flaminio, M. Fletcher, H. Fong, J. D. Fournier, S. Frasca, F. Frasconi, Z. Frei, A. Freise, R. Frey, V. Frey, P. Fritschel, V. V. Frolov, P. Fulda, M. Fyffe, H. A. Gabbard, J. R. Gair, L. Gammaitoni, S. G. Gaonkar, F. Garufi, G. Gaur, N. Gehrels, G. Gemme, P. Geng, E. Genin, A. Gennai, J. George, L. Gergely, V. Germain, A. Ghosh, A. Ghosh, S. Ghosh, J. A. Giaime, K. D. Giardina, A. Giazotto, K. Gill, A. Glaefke, E. Goetz, R. Goetz, L. Gondan, G. González, J. M. Gonzalez Castro, A. Gopakumar, N. A. Gordon, M. L. Gorodetsky, S. E. Gossan, M. Gosselin, R. Gouaty, A. Grado, C. Graef, P. B. Graff, M. Granata, A. Grant, S. Gras, C. Gray, G. Greco, A. C. Green, P. Groot, H. Grote, S. Grunewald, G. M. Guidi, X. Guo, A. Gupta, M. K. Gupta, K. E. Gushwa, E. K. Gustafson, R. Gustafson, J. J. Hacker, B. R. Hall, E. D. Hall, H. Hamilton, G. Hammond, M. Haney, M. M. Hanke, J. Hanks, C. Hanna, M. D. Hannam, J. Hanson, T. Hardwick, J. Harms, G. M. Harry, I. W. Harry, M. J. Hart, M. T. Hartman, C. J. Haster, K. Haughian, J. Healy, A. Heidmann, M. C. Heintze, H. Heitmann, P. Hello, G. Hemming, M. Hendry, I. S. Heng, J. Hennig, J. Henry, A. W. Heptonstall, M. Heurs, S. Hild, D. Hoak, D. Hofman, K. Holt, D. E. Holz, P. Hopkins, J. Hough, E. A. Houston, E. J. Howell, Y. M. Hu, S. Huang, E. A. Huerta, D. Huet, B. Hughey, S. Husa, S. H. Huttner, T. Huynh-Dinh, N. Indik, D. R. Ingram, R. Inta, H. N. Isa, J. M. Isac, M. Isi, T. Isogai, B. R. Iyer, K. Izumi, T. Jacqmin, H. Jang, K. Jani, P. Jaranowski, S. Jawahar, L. Jian, F. Jiménez-Forteza, W. W. Johnson, N. K. Johnson-McDaniel, D. I. Jones, R. Jones, R. J. Jonker, L. Ju, H. K, C. V. Kalaghatgi, V. Kalogera, S. Kandhasamy, G. Kang, J. B. Kanner, S. J. Kapadia, S. Karki, K. S. Karvinen, M. Kasprzack, E. Katsavounidis, W. Katzman, S. Kaufer, T. Kaur, K. Kawabe, F. Kéfélian, M. S. Kehl, D. Keitel, D. B. Kelley, W. Kells, R. Kennedy, J. S. Key, F. Y. Khalili, I. Khan, S. Khan, Z. Khan, E. A. Khazanov, N. Kijbunchoo, C. W. Kim, C. Kim, J. Kim, K. Kim, N. Kim, W. Kim, Y. M. Kim, S. J. Kimbrell, E. J. King, P. J. King, J. S. Kissel, B. Klein, L. Kleybolte, S. Klimenko, S. M. Koehlenbeck, S. Koley, V. Kondrashov, A. Kontos, M. Korobko, W. Z. Korth, I. Kowalska, D. B. Kozak, V. Kringel, B. Krishnan, A. Królak, C. Krueger, G. Kuehn, P. Kumar, R. Kumar, L. Kuo, A. Kutynia, B. D. Lackey, M. Landry, J. Lange, B. Lantz, P. D. Lasky, M. Laxen, A. Lazzarini, C. Lazzaro, P. Leaci, S. Leavey, E. O. Lebigot, C. H. Lee, H. K. Lee, H. M. Lee, K. Lee, A. Lenon, M. Leonardi, J. R. Leong, N. Leroy, N. Letendre, Y. Levin, J. B. Lewis, T. G. Li, A. Libson, T. B. Littenberg, N. A. Lockerbie, A. L. Lombardi, L. T. London, J. E. Lord, M. Lorenzini, V. Loriette, M. Lormand, G. Losurdo, J. D. Lough, C. O. Lousto, H. Lück, A. P. Lundgren, R. Lynch, Y. Ma, B. Machenschalk, M. MacInnis, D. M. Macleod, F. Magaña-Sandoval, L. Magaña Zertuche, R. M. Magee, E. Majorana, I. Maksimovic, V. Malvezzi, N. Man, I. Mandel, V. Mandic, V. Mangano, G. L. Mansell, M. Manske, M. Mantovani, F. Marchesoni, F. Marion, S. Márka, Z. Márka, A. S. Markosyan, E. Maros, F. Martelli, L. Martellini, I. W. Martin, D. V. Martynov, J. N. Marx, K. Mason, A. Masserot, T. J. Massinger, M. Masso-Reid, S. Mastrogiovanni, F. Matichard, L. Matone, N. Mavalvala, N. Mazumder, R. McCarthy, D. E. McClelland, S. McCormick, S. C. McGuire, G. McIntyre, J. McIver, D. J. McManus, T. McRae, S. T. McWilliams, D. Meacher, G. D. Meadors, J. Meidam, A. Melatos, G. Mendell, R. A. Mercer, E. L. Merilh, M. Merzougui, S. Meshkov, C. Messenger, C. Messick, R. Metzdorff, P. M. Meyers, F. Mezzani, H. Miao, C. Michel, H. Middleton, E. E. Mikhailov, L. Milano, A. L. Miller, A. Miller, B. B. Miller, J. Miller, M. Millhouse, Y. Minenkov, J. Ming, S. Mirshekari, C. Mishra, S. Mitra, V. P. Mitrofanov, G. Mitselmakher, R. Mittleman, A. Moggi, M. Mohan, S. R. Mohapatra, M. Montani, B. C. Moore, C. J. Moore, D. Moraru, G. Moreno, S. R. Morriss, K. Mossavi, B. Mours, C. M. Mow-Lowry, G. Mueller, A. W. Muir, A. Mukherjee, D. Mukherjee, S. Mukherjee, N. Mukund, A. Mullavey, J. Munch, D. J. Murphy, P. G. Murray, A. Mytidis, I. Nardecchia, L. Naticchioni, R. K. Nayak, K. Nedkova, G. Nelemans, T. J. Nelson, M. Neri, A. Neunzert, G. Newton, T. T. Nguyen, A. B. Nielsen, S. Nissanke, A. Nitz, F. Nocera, D. Nolting, M. E. Normandin, L. K. Nuttall, J. Oberling, E. Ochsner, J. O'Dell, E. Oelker, G. H. Ogin, J. J. Oh, S. H. Oh, F. Ohme, M. Oliver, P. Oppermann, R. J. Oram, B. O'Reilly, R. O'Shaughnessy, D. J. Ottaway, H. Overmier, B. J. Owen, A. Pai, S. A. Pai, J. R. Palamos, O. Palashov, C. Palomba, A. Pal-Singh, H. Pan, C. Pankow, F. Pannarale, B. C. Pant, F. Paoletti, A. Paoli, M. A. Papa, H. R. Paris, W. Parker, D. Pascucci, A. Pasqualetti, R. Passaquieti, D. Passuello, B. Patricelli, Z. Patrick, B. L. Pearlstone, M. Pedraza, R. Pedurand, L. Pekowsky, A. Pele, S. Penn, A. Perreca, L. M. Perri, H. P. Pfeiffer, M. Phelps, O. J. Piccinni, M. Pichot, F. Piergiovanni, V. Pierro, G. Pillant, L. Pinard, I. M. Pinto, M. Pitkin, M. Poe, R. Poggiani, P. Popolizio, A. Post, J. Powell, J. Prasad, V. Predoi, T. Prestegard, L. R. Price, M. Prijatelj, M. Principe, S. Privitera, R. Prix, G. A. Prodi, L. Prokhorov, O. Puncken, M. Punturo, P. Puppo, M. Pürrer, H. Qi, J. Qin, S. Qiu, V. Quetschke, E. A. Quintero, R. Quitzow-James, F. J. Raab, D. S. Rabeling, H. Radkins, P. Raffai, S. Raja, C. Rajan, M. Rakhmanov, P. Rapagnani, V. Raymond, M. Razzano, V. Re, J. Read, C. M. Reed, T. Regimbau, L. Rei, S. Reid, D. H. Reitze, H. Rew, S. D. Reyes, F. Ricci, K. Riles, M. Rizzo, N. A. Robertson, R. Robie, F. Robinet, A. Rocchi, L. Rolland, J. G. Rollins, V. J. Roma, J. D. Romano, R. Romano, G. Romanov, J. H. Romie, D. Rosińska, S. Rowan, A. Rüdiger, P. Ruggi, K. Ryan, S. Sachdev, T. Sadecki, L. Sadeghian, M. Sakellariadou, L. Salconi, M. Saleem, F. Salemi, A. Samajdar, L. Sammut, E. J. Sanchez, V. Sandberg, B. Sandeen, J. R. Sanders, B. Sassolas, B. S. Sathyaprakash, P. R. Saulson, O. E. Sauter, R. L. Savage, A. Sawadsky, P. Schale, R. Schilling, J. Schmidt, P. Schmidt, R. Schnabel, R. M. Schofield, A. Schönbeck, E. Schreiber, D. Schuette, B. F. Schutz, J. Scott, S. M. Scott, D. Sellers, A. S. Sengupta, D. Sentenac, V. Sequino, A. Sergeev, Y. Setyawati, D. A. Shaddock, T. Shaffer, M. S. Shahriar, M. Shaltev, B. Shapiro, P. Shawhan, A. Sheperd, D. H. Shoemaker, D. M. Shoemaker, K. Siellez, X. Siemens, M. Sieniawska, D. Sigg, A. D. Silva, A. Singer, L. P. Singer, A. Singh, R. Singh, A. Singhal, A. M. Sintes, B. J. Slagmolen, J. R. Smith, N. D. Smith, R. J. Smith, E. J. Son, B. Sorazu, F. Sorrentino, T. Souradeep, A. K. Srivastava, A. Staley, M. Steinke, J. Steinlechner, S. Steinlechner, D. Steinmeyer, B. C. Stephens, S. P. Stevenson, R. Stone, K. A. Strain, N. Straniero, G. Stratta, N. A. Strauss, S. Strigin, R. Sturani, A. L. Stuver, T. Z. Summerscales, L. Sun, S. Sunil, P.

Optics EXPRESS

J. Sutton, B. L. Swinkels, M. J. Szczepańczyk, M. Tacca, D. Talukder, D. B. Tanner, M. Tápai, S. P. Tarabrin, A. Taracchini, R. Taylor, T. Theeg, M. P. Thirugnanasambandam, E. G. Thomas, M. Thomas, P. Thomas, K. A. Thorne, E. Thrane, S. Tiwari, V. Tiwari, K. V. Tokmakov, K. Toland, C. Tomlinson, M. Tonelli, Z. Tornasi, C. V. Torres, C. I. Torrie, D. Töyrä, F. Travasso, G. Traylor, D. Trifirò, M. C. Tringali, L. Trozzo, M. Tse, M. Turconi, D. Tuyenbayev, D. Ugolini, C. S. Unnikrishnan, A. L. Urban, S. A. Usman, H. Vahlbruch, G. Vajente, G. Valdes, M. Vallisneri, N. van Bakel, M. van Beuzekom, J. F. van den Brand, C. Van Den Broeck, D. C. Vander-Hyde, L. van der Schaaf, J. V. van Heijningen, A. A. van Veggel, M. Vardaro, S. Vass, M. Vasúth, R. Vaulin, A. Vecchio, G. Vedovato, J. Veitch, P. J. Veitch, K. Venkateswara, D. Verkindt, F. Vetrano, A. Viceré, S. Vinciguerra, D. J. Vine, J. Y. Vinet, S. Vitale, T. Vo, H. Vocca, C. Vorvick, D. V. Voss, W. D. Vousden, S. P. Vyatchanin, A. R. Wade, L. E. Wade, M. Wade, M. Walker, L. Wallace, S. Walsh, G. Wang, H. Wang, M. Wang, X. Wang, Y. Wang, R. L. Ward, J. Warner, M. Was, B. Weaver, L. W. Wei, M. Weinert, A. J. Weinstein, R. Weiss, L. Wen, P. Weßels, T. Westphal, K. Wette, J. T. Whelan, B. F. Whiting, R. D. Williams, A. R. Williamson, J. L. Willis, B. Willke, M. H. Wimmer, W. Winkler, C. C. Wipf, H. Wittel, G. Woan, J. Woehler, J. Worden, J. L. Wright, D. S. Wu, G. Wu, J. Yablon, W. Yam, H. Yamamoto, C. C. Yancey, H. Yu, M. Yvert, A. Zadrożny, L. Zangrando, M. Zanolin, J. P. Zendri, M. Zevin, L. Zhang, M. Zhang, Y. Zhang, C. Zhao, M. Zhou, Z. Zhou, X. J. Zhu, M. E. Zucker, S. E. Zuraw, J. Zweizig, M. Boyle, D. Hemberger, L. E. Kidder, G. Lovelace, S. Ossokine, M. Scheel, B. Szilagyi, and S. Teukolsky; LIGO Scientific Collaboration and Virgo Collaboration, "GW151226: Observation of gravitational waves from a 22-solar-mass binary black hole coalescence," Phys. Rev. Lett. **116**(24), 241103 (2016).

8. D. Robertson, C. Killow, H. Ward, J. Hough, G. Heinzel, A. Garcia, V. Wand, U. Johann, and C. Braxmaier, "LTP interferometer – noise sources and performance," Class. Quantum Gravity **22**(10), S155–S163 (2005).
9. M. Armano, H. Audley, G. Auger, J. T. Baird, M. Bassan, P. Binetruy, M. Born, D. Bortoluzzi, N. Brandt, M. Caleno, L. Carbone, A. Cavalleri, A. Cesarini, G. Ciani, G. Congedo, A. M. Cruise, K. Danzmann, M. de Deus Silva, R. De Rosa, M. Diaz-Aguiló, L. Di Fiore, I. Diepholz, G. Dixon, R. Dolesi, N. Dunbar, L. Ferraioli, V. Ferroni, W. Fichter, E. D. Fitzsimons, R. Flatscher, M. Freschi, A. F. García Marín, C. García Marirrodriga, R. Gerndt, L. Gesa, F. Gibert, D. Giardini, R. Giusteri, F. Guzmán, A. Grado, C. Grimani, A. Grynagier, J. Grzymisch, I. Harrison, G. Heinzel, M. Hewitson, D. Hollington, D. Hoyland, M. Hueller, H. Inchauspé, O. Jennrich, P. Jetzer, U. Johann, B. Johlander, N. Karnesis, B. Kaune, N. Korsakova, C. J. Killow, J. A. Lobo, I. Lloro, L. Liu, J. P. López-Zaragoza, R. Maarschalkerweerd, D. Mance, V. Martín, L. Martin-Polo, J. Martino, F. Martin-Porqueras, S. Madden, I. Mateos, P. W. McNamara, J. Mendes, L. Mendes, A. Monsky, D. Nicolodi, M. Nofrarias, S. Paczkowski, M. Perreur-Lloyd, A. Petiteau, P. Pivato, E. Plagnol, P. Prat, U. Ragnit, B. Raïs, J. Ramos-Castro, J. Reiche, D. I. Robertson, H. Rozemeijer, F. Rivas, G. Russano, J. Sanjuán, P. Sarra, A. Schleicher, D. Shaul, J. Slutsky, C. F. Sopuerta, R. Stanga, F. Steier, T. Sumner, D. Texier, J. I. Thorpe, C. Trenkel, M. Tröbs, H. B. Tu, D. Vetrugno, S. Vitale, V. Wand, G. Wanner, H. Ward, C. Warren, P. J. Wass, D. Wealthy, W. J. Weber, L. Wissel, A. Wittchen, A. Zambotti, C. Zanoni, T. Ziegler, and P. Zweifel, "Sub-femto-g free fall for space-based gravitational wave observatories: LISA pathfinder results," Phys. Rev. Lett. **116**(23), 231101 (2016).
10. B. Willke, P. Aufmuth, C. Aulbert, S. Babak, R. Balasubramanian, B. W. Barr, S. Berukoff, S. Bose, G. Cagnoli, M. M. Casey, D. Churches, D. Clubley, C. N. Colacino, D. R. M. Crooks, C. Cutler, K. Danzmann, R. Davies, R. Dupuis, E. Elliffe, C. Fallnich, A. Freise, S. Goßler, A. Grant, H. Grote, G. Heinzel, A. Heptonstall, M. Heurs, M. Hewitson, J. Hough, O. Jennrich, K. Kawabe, K. Kötter, V. Leonhardt, H. Lück, M. Malec, P. W. McNamara, S. A. McIntosh, K. Mossavi, S. Mohanty, S. Mukherjee, S. Nagano, G. P. Newton, B. J. Owen, D. Palmer, M. A. Papa, M. V. Plissi, V. Quetschke, D. I. Robertson, N. A. Robertson, S. Rowan, A. Rüdiger, B. S. Sathyaprakash, R. Schilling, B. F. Schutz, R. Senior, A. M. Sintes, K. D. Skeldon, P. Sneddon, F. Stief, K. A. Strain, I. Taylor, C. I. Torrie, A. Vecchio, H. Ward, U. Weiland, H. Welling, P. Williams, W. Winkler, G. Woan, and I. Zawischa, "The GEO 600 gravitational wave detector," Class. Quantum Gravity **19**(7), 1377–1387 (2002).
11. D.-H. Gwo, "Ultra-precision bonding for cryogenic fused-silica optics," Proc. SPIE **3435**, 136–142 (1998).
12. V. Greco, F. Marchesini, and G. Molesini, "Optical contact and van der Waals interactions: the role of the surface topography in determining the bonding strength of thick glass plates," J. Opt. A, Pure Appl. Opt. **3**(1), 85–88 (2001).
13. J. Haisma and G. A. C. M. Spierings, "Contact bonding, including direct-bonding in a historical and recent context of materials science and technology, physics and chemistry," Mater. Sci. Eng. Rep. **37**(1–2), 1–60 (2002).
14. B. Bhushan, *Springer Handbook of Nanotechnology* (Springer Science & Business Media, 2004), Vol. 1.
15. R. Knechtel, "Glass frit bonding: an universal technology for wafer level encapsulation and packaging," Microsyst. Technol. **12**(1–2), 63–68 (2005).
16. K. Nötzold, C. Dresbach, J. Graf, and B. Böttge, "Temperature dependent fracture toughness of glass frit bonding layers," Microsyst. Technol. **16**(7), 1243–1249 (2010).
17. J. Haisma, N. Hattu, J. T. Pulles, E. Steding, and J. C. Vervest, "Direct bonding and beyond," Appl. Opt. **46**(27), 6793–6803 (2007).
18. S. Sinha, K. E. Urbanek, A. Krzywicki, and R. L. Byer, "Investigation of the suitability of silicate bonding for facet termination in active fiber devices," Opt. Express **15**(20), 13003–13022 (2007).
19. D.-H. Gwo, "Ultra-precision and reliable bonding method," U.S. Patent **US 6284085 B1**, 1–18 (2001).
20. D.-H. Gwo, "Hydroxide-catalyzed bonding," U.S. Patent **US 6548176 B1**, 1–40 (2003).
21. H. S. Kim and T. L. Schmitz, "Shear strength evaluation of hydroxide catalysis bonds for glass–glass and glass–aluminum assemblies," Precis. Eng. **37**(1), 23–32 (2013).

Optics EXPRESS

22. E. J. Elliffe, J. Bogenstahl, A. Deshpande, J. Hough, C. Killow, S. Reid, D. Robertson, S. Rowan, H. Ward, and G. Cagnoli, "Hydroxide-catalysis bonding for stable optical systems for space," Class. Quantum Gravity **22**(10), S257–S267 (2005).
23. S. Rowan, S. M. Twyford, J. Hough, D.-H. Gwo, and R. Route, "Mechanical losses associated with the technique of hydroxide-catalysis bonding of fused silica," Phys. Lett. A **246**(6), 471–478 (1998).
24. P. H. Sneddon, S. Bull, G. Cagnoli, D. R. M. Crooks, E. J. Elliffe, J. E. Faller, M. M. Fejer, J. Hough, and S. Rowan, "The intrinsic mechanical loss factor of hydroxy-catalysis bonds for use in the mirror suspensions of gravitational wave detectors," Class. Quantum Gravity **20**(23), 5025–5037 (2003).
25. A. A. van Veggel, J. Scott, D. A. Skinner, B. Bezensek, W. Cunningham, J. Hough, I. Martin, P. Murray, S. Reid, and S. Rowan, "Strength testing and SEM imaging of hydroxide-catalysis bonds between silicon," Class. Quantum Gravity **26**(17), 175007 (2009).
26. N. L. Beveridge, A. A. van Veggel, M. Hendry, P. Murray, R. A. Montgomery, E. Jesse, J. Scott, R. B. Bezensek, L. Cunningham, J. Hough, R. Nawrodt, S. Reid, and S. Rowan, "Low-temperature strength tests and SEM imaging of hydroxide catalysis bonds in silicon," Class. Quantum Gravity **28**(22), 229501 (2011).
27. K. A. Haughian, *Aspects of Materials Research for Advanced and Future Generations of Gravitational Wave Detectors* (PhD thesis, University of Glasgow, 2012)
28. A. Dari, F. Travasso, H. Vocca, and L. Gammaitoni, "Breaking strength tests on silicon and sapphire bondings for gravitational wave detectors," Class. Quantum Gravity **27**(4), 045010 (2010).
29. A. A. van Veggel, D. van den Ende, J. Bogenstahl, S. Rowan, W. Cunningham, G. H. M. Gubbels, and H. Nijmeijer, "Hydroxide catalysis bonding of silicon carbide," J. Eur. Ceram. Soc. **28**(1), 303–310 (2008).
30. R. Douglas, A. A. van Veggel, L. Cunningham, K. Haughian, J. Hough, and S. Rowan, "Cryogenic and room temperature strength of sapphire jointed by hydroxide-catalysis bonding," Class. Quantum Gravity **31**(4), 045001 (2014).
31. S. Rowan, J. Hough, and E. J. Elliffe, "Silicon carbide bonding," U.S. Patent **US 2007/0221326 A1**, 1–6 (2007).
32. D. A. van den Ende and G. H. M. Gubbels, "Fracture toughness of hydroxide catalysis bonds between silicon carbide and Zerodur low thermal expansion glass-ceramic," Mater. Chem. Phys. **143**(3), 1236–1242 (2014).
33. O. S. Heavens, *Optical Properties of Thin Solid Films* (Dover Publications Inc., 1991).
34. J. R. Taylor, *An Introduction to Error Analysis: The Study of Uncertainties in Physical Measurements* (University Science Books, 1997).
35. A. Preston, B. Balaban, and G. Mueller, "Hydroxide-bonding strength measurements for space-based optical missions," Int. J. Appl. Ceram. Technol. **5**(4), 365–372 (2008).
36. D. Tentori-Santa-Cruz and J. R. Lerma, "Refractometry by minimum deviation: accuracy analysis," Opt. Eng. **29**(2), 160–168 (1990).

1. Introduction

In this paper a non-destructive technique for determining the refractive index and thickness of hydroxide-catalysis bonds from reflectivity measurements is reported. This technique strikes two birds with one stone:

1) it will be invaluable for enabling us to tailor the optical properties of hydroxide-catalysis bonds for optical applications such as fabrication of high power laser crystals assembled using hydroxide-catalysis bonding [1] and optical fibre injection components [2], in which low reflectivity is required;

2) it could give in situ measurements of bond thickness in the mirror suspensions of ground-based gravitional wave detectors to more accurately predict the thermal noise from these bonds in these suspensions [3].

Jointing materials is inevitable in the realization of many high performance devices. There is an ever increasing demand, both from industry and academic research, for reliable, easy, inexpensive techniques for precisely jointing components where the bonds possess high strength with the required levels of reflection and absorption amongst other properties [4].

Hydroxide-catalysis bonding is such a technique which has been instrumental in the assembly of opto-mechanical parts of the recently extremely successful aLIGO gravitational wave detectors (in the extremely low thermal noise mirror suspensions [5]) which recently made the first two direct detections of gravitational waves both caused by two black holes merging [6,7]; as well as the ultrastable interferometer readout system [8] of the successful LISA Pathfinder mission of which results were also reported recently [9]. Besides these applications this technique had already been pioneered in the extremely low thermal noise mirror suspensions of the GEO600 [10] gravitational wave detector and in the star tracker telescope of the Gravity Probe B mission which operated in vacuum at 2.5 K [11].

Optics EXPRESS

This technique has however only really been applied in a mechanical sense, not in an optical sense, though these bonds are transparent to the eye and could therefore be interesting for applications in which a thin optically transparent and mechanically strong joint between optical components is required and other techniques (e.g. optical contacting [12,13], epoxy bonding [14], frit bonding [15,16] and direct bonding [13,17]) may not be ideal.

Initial research and development has started for the use of hydroxide-catalysis bonding in laser systems [18]. In this paper, first measurements of the reflectivity of a hydroxide-catalysis bonds between silica substrates (using sodium silicate solution) were presented giving a value less than $7.08 \cdot 10^{-4}$ at normal incidence: these bonds were resistant to 70 J/cm^2 of laser power for 25 ns pulses at a wavelength of 1064 nm. These first results make this technique highly attractive for further development of optical applications, such as fabrication of high power laser crystals assembled using hydroxide-catalysis bonding [1] and optical fibre injection components [2].

In this paper the method of taking reflectivity measurements and then extracting the information on the bond thickness and refractive index from hydroxide-catalysis bonds is explained as well as a demonstration of the technique through measurements of reflectivity of a hydroxide-catalysis bond between two silica windows as a function of curing time.

2. What is hydroxide-catalysis bonding?

Hydroxide-catalysis or 'silicate' bonding is a jointing technique that was patented by Gwo [19,20] at Stanford University and used in the construction of an all-fused-silica star tracking telescope for the Gravity Probe B satellite-based mission [11]. An aqueous hydroxide solution (typically containing sodium or potassium hydroxide) is placed between two surfaces, which initiates a chemical reaction with polymer-like chains being formed (siloxane chains in the case of a silica based substrate), jointing the two surfaces together. The by-product of the process is water which slowly migrates out of the bond. Destructive strength tests on silica samples have shown that the bond strength increases with curing time and after approximately four weeks it reaches a maximum value [21]: after only a few hours from the start of the jointing process the bond has sufficient strength to allow the bonded sample to be handled [20–23]. More details on the chemistry can be found in [19,20]. The materials can be jointed at room temperature, realising extremely thin [20,24–26], low mechanical loss [3,23,24] and high strength bonds [20,25–30] with high precision alignment [8,11].

It is possible to use this technique to bond other materials provided that a silicate-like network can be formed between surfaces to be jointed. This is the case for most oxide and oxidisable materials, such as for example fused silica [11,20], silicon [25,26,28], silicon carbide [29,31,32] and sapphire [24,28,30].

3. Method to determine refractive index and thickness of a bond from optical reflectivity measurements

3.1 Optical set-up

The optical assembly (Fig. 1) was composed of a green laser diode module (λ = 532 nm, maximum output power </~1 mW, 1/e^2 diameter of 0.9 mm with a divergence of ~0.2 mrad); a half wave plate together with a polarizing beamsplitter cube to fix the polarisation of the laser light; another half wave plate to allow selection of the perpendicular ($\perp$) and parallel ($\parallel$) polarisations of the incident light; a glass plate to allow a small fraction of the light to be sent to photodiode 1 (2.75 x 2.75 mm sensitive area) to monitor any fluctuations in intensity of the probe beam; the sample on a rotation mount from which the light can be reflected at a range of angles of incidence and photodiode 2 to measure the intensity of the reflected beam. The photodiode 2 ($\varnothing$ 2.5 mm sensitive area) and pinhole were rotated together around the sample on a square gridded breadboard, making sure the beam was at normal angle of incidence to the photodiode surface and (as much as possible) at constant distance from the sample at all angles measured (though this was not critical due to the low beam divergence).

Optics EXPRESS

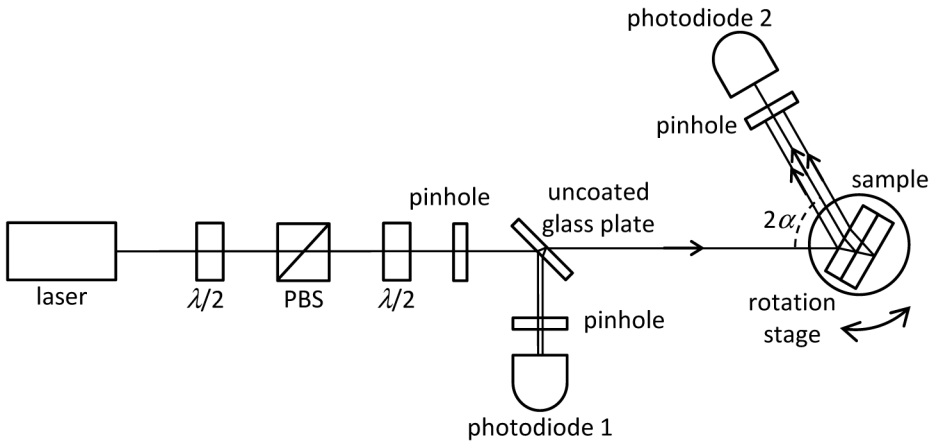

Fig. 1. Schematic diagram of the setup used to measure the reflectivity of bonded interfaces.

When the laser beam is incident on the sample, three reflected spots are produced due to the light reflected at the front, bonded and back surfaces of the bonded sample: the pinholes (4 mm diameter) aid with alignment, minimizes stray light and allows separation of the beam spot from the bonded interface from the other reflected beams.

The power of the incident and reflected laser beams were measured by means of respective photodiodes for a range of angles of incidence α. The angle of incidence was varied by rotating the sample on a rotation stage (Fig. 1). These measurements were carried out for the $\perp$ and $\parallel$ polarisations of the laser beam. From the ratio between the reflected and incident powers V_{output} and V_{input} (measured in Volts using the photodiodes with a current to voltage amplifier circuit), reflectances for $\perp$ and $\parallel$ polarized light, $R_\perp$ and $R_\parallel$ respectively, can be determined:

$$\begin{aligned} R_\perp &= V_{output,\perp} / V_{input,\perp} \\ R_\parallel &= V_{output,\parallel} / V_{input,\parallel}. \end{aligned} \tag{1}$$

Measurements on both photodiodes were always taken simultaneously to cancel out any errors caused by fluctuations of laser power in the reflectance

As the power of light incident on photodiode 1 is not the power of light actually incident on the sample, measurements were performed in advance to determine the conversion factor k at both $\perp$ and $\parallel$ polarisation, so that $V_{input,\perp} = k_\perp \cdot V_{photodiode1}$ and $V_{input,\parallel} = k_\parallel \cdot V_{photodiode1}$. This was determined for a range of light power levels and several different days and it was found that $k_\perp = 4.92 \pm 0.02$ and $k_\parallel = 56.11 \pm 1.10$.

3.2 Optical model

In order to obtain the refractive index and thickness of a hydroxide-catalysis bond from the measurements of reflectance, the experimental data has to be compared with that obtained from a theoretical model.

Optics EXPRESS

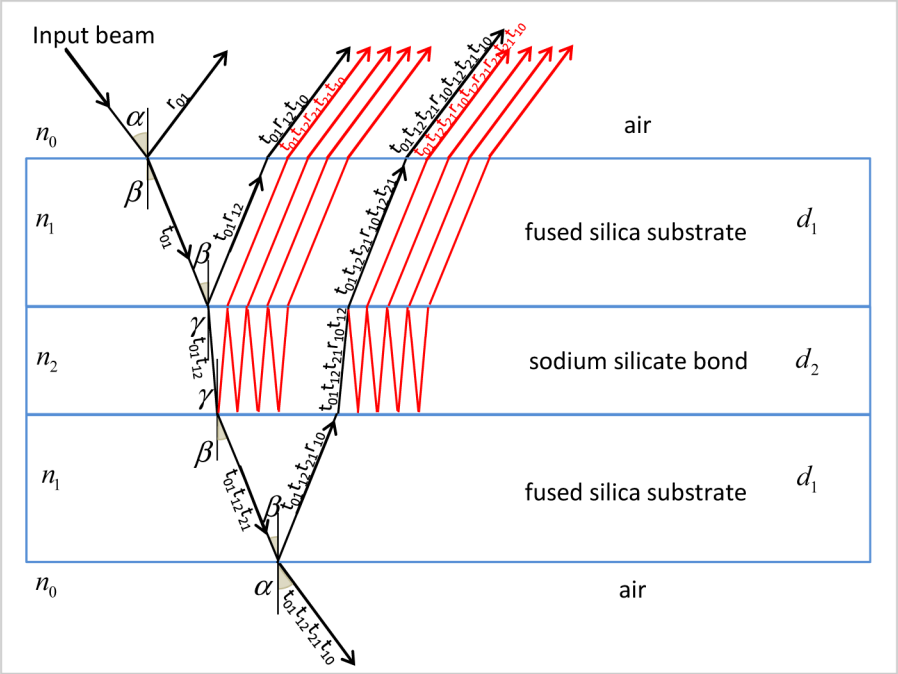

Fig. 2. Schematic diagram of bonded sample (not to scale). Two discs of fused silica are joined by hydroxide-catalysis bonding.

The model is based on the arrangement shown in Fig. 2 and assumes the substrates and bond material are isotropic media.

The amplitude of the reflection and transmission coefficients, r and t, for each boundary between media of different refractive index are shown. For example, r_{01} is the fraction of the amplitude of the incident light reflected at the interface between the medium with refractive index n_0 and that with refractive index n_1.

In this model the effects of thin film interference are also included and the following relationships for reflectances for the $\perp$ and $\parallel$ polarisation components of the incident light can be deduced for the bond layer [33]:

$$R_{2,\perp} = \frac{2\left(1-r_{01,\perp}^2\right)^2 r_{12,\perp}^2 (1-\cos 2\delta_2)}{1-2r_{12,\perp}^2 \cos 2\delta_2 + r_{12,\perp}^4}$$
$$R_{2,\parallel} = \frac{2\left(1-r_{01,\parallel}^2\right)^2 r_{12,\parallel}^2 (1-\cos 2\delta_2)}{1-2r_{12,\parallel}^2 \cos 2\delta_2 + r_{12,\parallel}^4}, \quad (2)$$

where the reflection coefficients are:

Optics EXPRESS

$$
\begin{aligned}
r_{01,\perp} &= \frac{\cos\alpha - \left((n_1/n_0)^2 - (\sin\alpha)^2\right)^{1/2}}{\cos\alpha + \left((n_1/n_0)^2 - (\sin\alpha)^2\right)^{1/2}} \\
r_{01,\parallel} &= \frac{(n_1/n_0)^2\cos\alpha - \left((n_1/n_0)^2 - (\sin\alpha)^2\right)^{1/2}}{(n_1/n_0)^2\cos\alpha + \left((n_1/n_0)^2 - (\sin\alpha)^2\right)^{1/2}} \\
r_{12,\perp} &= \frac{\cos\beta - \left((n_2/n_1)^2 - (\sin\beta)^2\right)^{1/2}}{\cos\beta + \left((n_2/n_1)^2 - (\sin\beta)^2\right)^{1/2}} \\
r_{12,\parallel} &= \frac{(n_2/n_1)^2\cos\beta - \left((n_2/n_1)^2 - (\sin\beta)^2\right)^{1/2}}{(n_2/n_1)^2\cos\beta + \left((n_2/n_1)^2 - (\sin\beta)^2\right)^{1/2}},
\end{aligned}
\tag{3}
$$

where

$$\beta = \arcsin((n_0/n_1)\sin\alpha) \tag{4}$$

and δ_2, which considers the change in phase of the beam on traversing the film, is:

$$\delta_2 = (2\pi/\lambda)n_2 d_2\left(1 - ((n_0/n_2)\sin\alpha)\right)^2. \tag{5}$$

Equations (2)–(5), obtained for the reflectances of the bond, are functions of the angle of incidence, the refractive indices of the various media, thickness of the bond layer and wavelength of the light source used. The angle of incidence is varied during the measurements (independent variable), the refractive indices of the air and the fused silica substrate are known (see details in the subsection 4.3), as well as the wavelength of laser (λ = 532 nm). As the refractive index and thickness of the bond are not known, it is necessary to define a method to find them.

3.3 Analysis: Bayesian likelihood

A Bayesian likelihood analysis code was written in Matlab, based on the least squares method [30] to find the refractive index and thickness of the bond.

For a grid of n_2 and d_2 possible combinations, the theoretical reflectances $R_\perp$ and $R_\parallel$ (Eq. (2)) are calculated and are then compared to the experimental reflectances (for a specific curing time) obtained by means of the setup.

If a Gaussian distribution of probability is assumed, the total normalized probability is given by [34]:

$$P = \exp\left[-\frac{1}{2}\left(\chi_\perp^2 + \chi_\parallel^2 - \chi_{\min}^2\right)\right], \tag{6}$$

where $\chi_k^2 = \sum_{i=1}^{n}\left(R_i^{th} - R_i^{\exp}\right)^2 \Big/ \sigma_{\exp,i}^2$ with $k = (\perp;\ \parallel)$, the theoretical reflectance R_i^{th} expressed by the Eqs. (2)–(4), the measured reflectance $R_i^{\exp}$ and its statistical error $\sigma_{\exp,i}$, and the minimum value $\chi_{\min}^2$ of the quantity $\left(\chi_\perp^2 + \chi_\parallel^2\right)$.

If n_2, d_2 and P are plotted on the x-axis, y-axis and z-axis respectively, a volume of probability is obtained. This volume can be intersected by planes of reliability, obtaining three confidence levels at 1σ, 2σ and 3σ, which correspond, respectively, to probabilities of 68%, 95% and 99%.

Optics EXPRESS

4. Case study: hydroxide-catalysis bond between two fused silica discs

4.1 Sample preparation

Two precision uncoated fused silica windows were procured from Edmund Optics Inc. (stock no. 47-836) with thickness and diameter of (5.0 ± 0.1) mm and ($50.0^{+0.0}_{-0.2}$) mm, respectively.

The flatness of the bonding surfaces of these windows was measured using a ZYGO GPI XP/D laser interferometer: it was found that the bonding surfaces had a flatness of 120 and 160 nm peak-to-valley respectively. Since the orientation of the two samples that were bonded was noted, it was possible to sum their maps and thus give the minimum relative separation between the bonding surfaces of two discs assuming physical contact in just three locations. This is shown in Fig. 3. Letters L, C and R indicate the locations at which later the reflectances were measured.

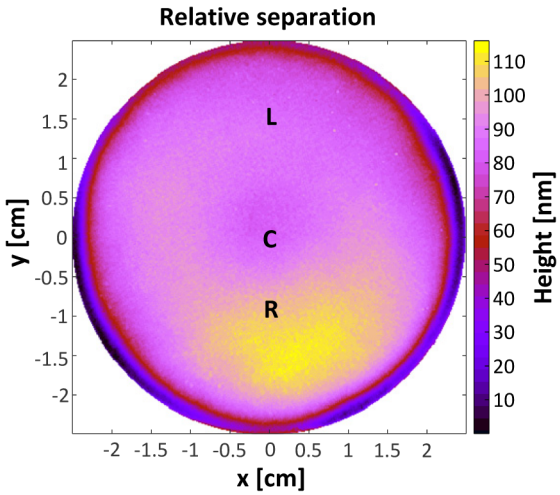

Fig. 3. Relative separation between two bonding surfaces of discs bonded by hydroxide-catalysis bonding.

Prior to bonding, the two discs were cleaned to ensure that no particles or films were present on the surfaces to be bonded: a regime involving cerium oxide and de-ionised (DI) water paste, bicarbonate of soda and DI water paste and methanol (details of this technique are discussed in [29,35]). The discs were bonded (Fig. 4) using sodium silicate solution.

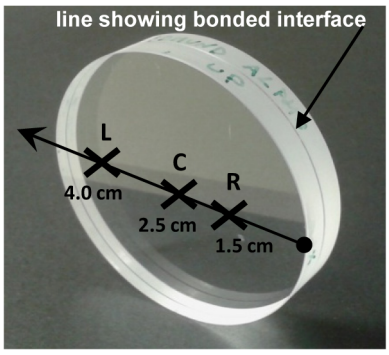

Fig. 4. Photograph of a pair of fused silica discs that were bonded by hydroxide-catalysis bonding, with three measurement locations shown.

Optics EXPRESS

Sodium silicate solution was chosen to allow a direct comparison of the reflectivity, refractive index and thickness of a bond reported in this paper to studies of bond properties performed in other research [3,20,24,27].

The bonding solution was made by diluting 2 ml of sodium silicate solution (Sigma-Aldrich Co. LLC.) with 12 ml of de-ionised water (a volumetric ratio of 1:6) and 15.7 µl (0.8 µl/cm^2 as used in aLIGO) of solution was pipetted onto one of the discs and the other disc was placed on top. The samples bond within a few minutes (etching and polymerisation stage), but curing (dehydration stage) in air at room temperature takes 4 weeks to reach full strength.

4.2 Reflectivity measurements

The reflectances of this sample were measured for three different positions on the front surface (locations 'L', 'C' and 'R' in Fig. 4) at a number of different time intervals after bonding. In this way the effect of curing time on the refractive index and thickness of bond could be studied, as well as the spatial homogeneity of these properties. Plots of measured reflectivity for both polarisations and all three positions as a function of angle of incidence (α) are shown in Fig. 5 (position 'L'), Fig. 6 (position 'C') and Fig. 7 (position 'R').

For both polarisations and for the three locations on the surface, it is observed that the values of bond reflectances are all less than 1%.

Initially the reflectance values fluctuate. During this phase, the reflectivity values do not follow a well-defined trend over the curing time. For the data taken at the positions marked 'L' and 'R' on the sample, this 'adjustment' phase lasts up to the 14th day, whereas for the position 'C', it is observed up to 11th day (look at the dark blue, red and green data points in Figs. 5, 6 and 7). After this period, the reflectivity steadily starts to drop as curing time increases. This implies that the centre settled before the areas near edges. After about three months, the reflectivity values are less than 0.1% for all locations and angles of incidence.

The different magnitude of reflectivity found between the three positions 'L', 'C' and 'R' can be influenced by the surface profile of the bonded interfaces. As discussed previously, the bonding surfaces of discs are not uniformly flat and it is therefore likely the bond thickness varies with location.

In Figs. 5, 6 and 7, the error bars for the measured angles of incidence and reflectances are also shown.

The principal source of error for the angle of incidence α is a random error introduced during initial alignment of the set-up for each measurement day, equal to ± 0.2°. The error in the reflectances measured is determined by the formula of propagation of uncertainty (Eq. (7)):

$$\sigma(R) = |R| \cdot \sqrt{\left(\sigma(V_{output})/V_{output}\right)^2 + \left(\sigma(V_{input})/V_{input}\right)^2} \tag{7}$$

where the correlation coefficient between V_{output} and V_{input} was considered equal to zero for both $\perp$ and $\parallel$ polarisation. The error is calculated separately for $\perp$ and $\parallel$ polarisation.

Optics EXPRESS

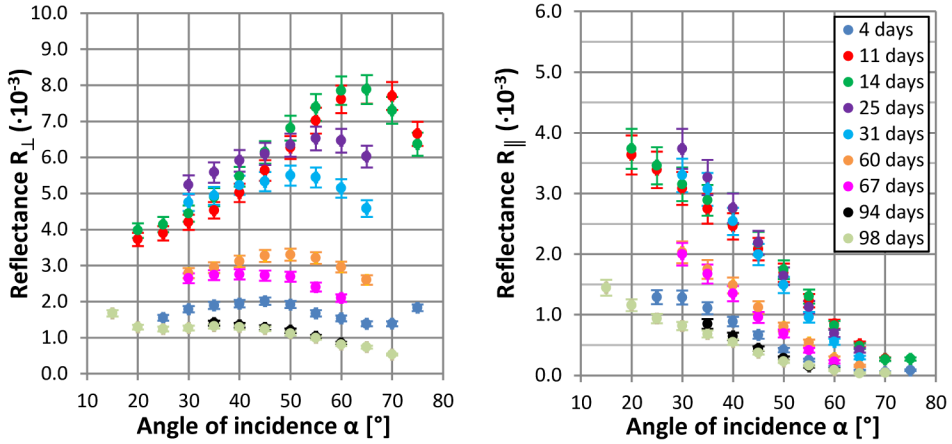

Fig. 5. Measured reflectances for ⊥ (left) and ∥ (right) polarisation plotted as a function of the angle of incidence α for the position 'L'. In the legend, the curing time is reported.

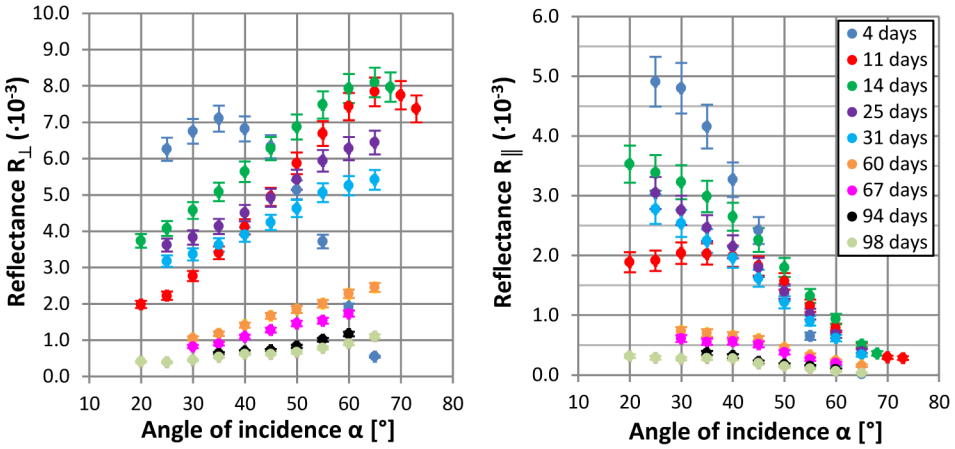

Fig. 6. Measured reflectances for ⊥ (left) and ∥ (right) polarisation plotted as a function of the angle of incidence α for the position 'C'. In the legend, the curing time is reported.

Optics EXPRESS

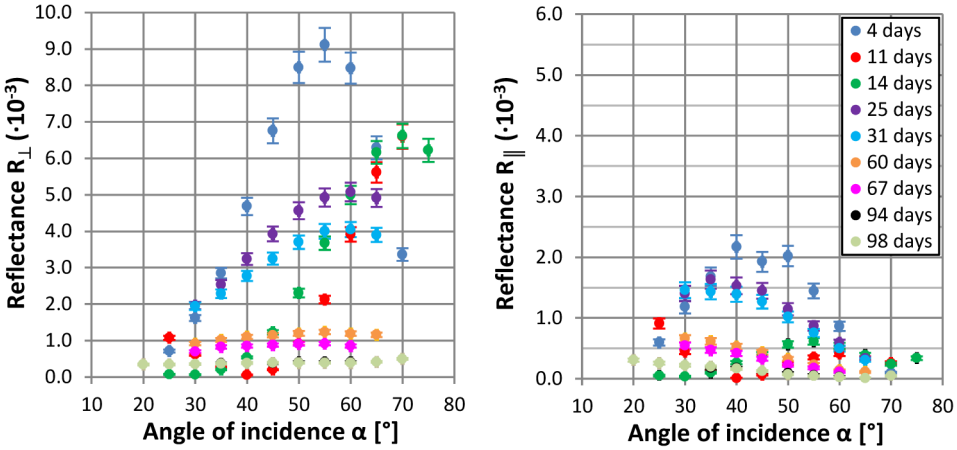

Fig. 7. Measured reflectances for ⊥ (left) and ∥ (right) polarisation plotted as a function of the angle of incidence α for the position 'R'. In the legend, the curing time is reported.

The error on V_{output}, $\sigma(V_{output})$, was determined from the statistical random variation of $V_{output,100}$ collected from the photodiode 2 circuitry (Fig. 1) and the estimation of the proportional factor F between different sensitivity levels of photodiodes themselves as the signal at photodiode 2 was measured with a sensitivity of 100 mV/μA whereas the signal at photodiode 1 was measured with a sensitivity of 10 mV/ μA. $\sigma(V_{output})$ could then be calculated using Eq. (8):

$$\sigma(V_{output}) = \sqrt{\left(\sigma(V_{output,100})/F\right)^2 + \left((V_{output,100})\cdot\sigma(F)/F^2\right)^2} \qquad (8)$$

The statistical random variation of $V_{output,100}$ is caused both by noise of the circuitry and power fluctuations of the laser and was determined by monitoring bond reflection power at 45° angle of incidence over a representative period of 20 minutes at both polarizations and repeated on several different days. It was calculated to be $\sigma(V_{output,100})$ = 0.20 mV and independent of polarization. Factor F was determined by measuring a large range of light powers at both 10 mV/ μA and 100 mV/ μA and repeating this on several days. It was found that F = 10.12 and $\sigma(F)$ = 0.49.

The error on V_{input}, $\sigma(V_{input})$, was obtained from the deviation from the linearity between voltages measured for both detectors for different light powers, and it was estimated to be 21.99 mV for ⊥ and 116.18 mV for ∥ polarisation. The different order of magnitude between the two polarisations is due to the greater uncertainty in measuring the voltages collected from the photodiode 1 circuitry as the intensity of the light reflected from the uncoated glass plate (Fig. 1) is much lower for ∥ polarisation than for ⊥ polarisation.

The setup as described here based on these calculations had a sensitivity of reflectance levels down to $2\cdot10^{-5}$ (or 0.002%), though at these levels other effects such as stray light become dominant.

4.3 Analysis results: refractive index and thickness

In the analysis of the data the following values were used:

- Each of the two discs has refractive index n_1 of 1.48 and thickness d_1 of 0.5 cm. The value of 1.48 ± 0.01 was obtained experimentally from measurements of Brewster's angle for the substrates ($\vartheta_B = \arctan(n_1/n_0)$, where the index of the air n_0 is approximated by 1).
- The grid of values for the bond layer (n_2 and d_2) was set, where the bond refractive index varied with 0.001 steps between 1.30 and 1.48 (not less than water (roughly),

Optics EXPRESS

not more than fused silica), and the bond thickness between 0 nm and 700 nm with 1 nm steps.

In Fig. 8 an example is shown for the results obtained for measurements of reflectivity carried out at the position marked 'L' on the sample: on the left of the figure, the three confidence levels of probability obtained from the Bayesian analysis at one specific curing time, and on the right, the comparison between experimental data and theoretical model for both polarisations of the incident light.

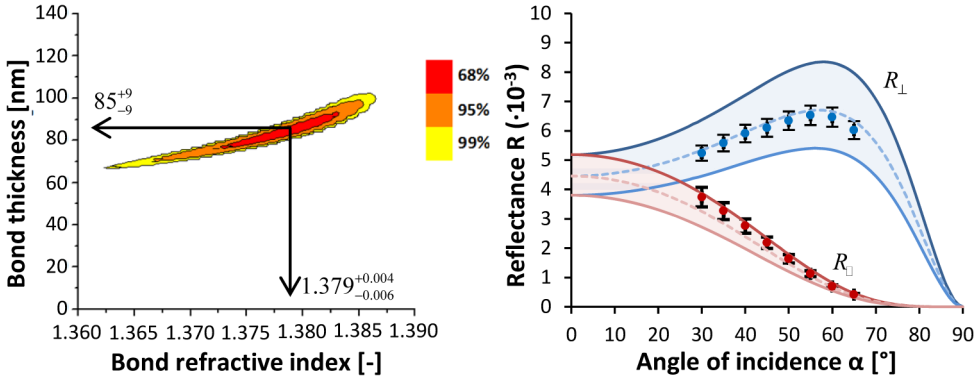

Fig. 8. Left: three confidence levels of probability. Right: measured data (dots) with their corresponding measurement 68% error bars and theoretical curves for the bond thickness and refractive index value found (for the dotted lines d_2 = 85 nm and n_2 = 1.379, the solid lines are for d_2 = 76 nm and n_2 = 1.373 and for d_2 = 94 nm and n_2 = 1.383). This is for the measurement done 25 days after bonding at the 'L' position on the sample.

From the confidence levels of probability, the constraints on parameters can be obtained and, in this case, are found to be consistent with a model where n_2 and d_2 are, respectively, $1.379^{+0.004}_{-0.006}$ and 85^{+9}_{-9} nm (Fig. 8, left).

In Fig. 9, the refractive index n_2 (top diagram) and thickness d_2 (bottom diagram) values, obtained from Bayesian likelihood analysis of each reflectivity measurement, are plotted as a function of the curing time for the three positions (see Fig. 4). For some data points two solutions were found one of which (filled data points) had a higher probability than the other (unfilled data points). This is due to the fact that the cosine function in the Eq. (2) can have more than one solution. As can be seen in the Fig. 9 this has a larger effect on the bond thickness than on the refractive index as the two solutions found for refractive index generally overlap whereas the two solutions found for bond thickness can be very different.

The top diagram in Fig. 9 shows an increasing trend of the refractive index for all three measurement locations starting at around n_2 equalling 1.37 at 4 days of curing and steadily increasing to 1.44 ± 0.01 at 98 days of curing. These results are in agreement with logical expectations: as the byproduct of the chemical reaction in hydroxide-catalysis bonding, water, migrates out of the bond (through evaporation or absorption into the bulk material) the silicate will become denser and more like fused silica.

The refractive index of the bonding solution (at the time of bonding) was measured to be 1.344 ± 0.001 (using minimum deviation refractometry [36]) which is just below the value found for 4 days of curing.

Note that, for the 'R' position, the values of n_2 at 94 and 98 days of curing drop, which are also characterised by greater error bars. These values are less accurate than the other measurements due to the reflectance levels approaching the setup sensitivity.

Optics EXPRESS

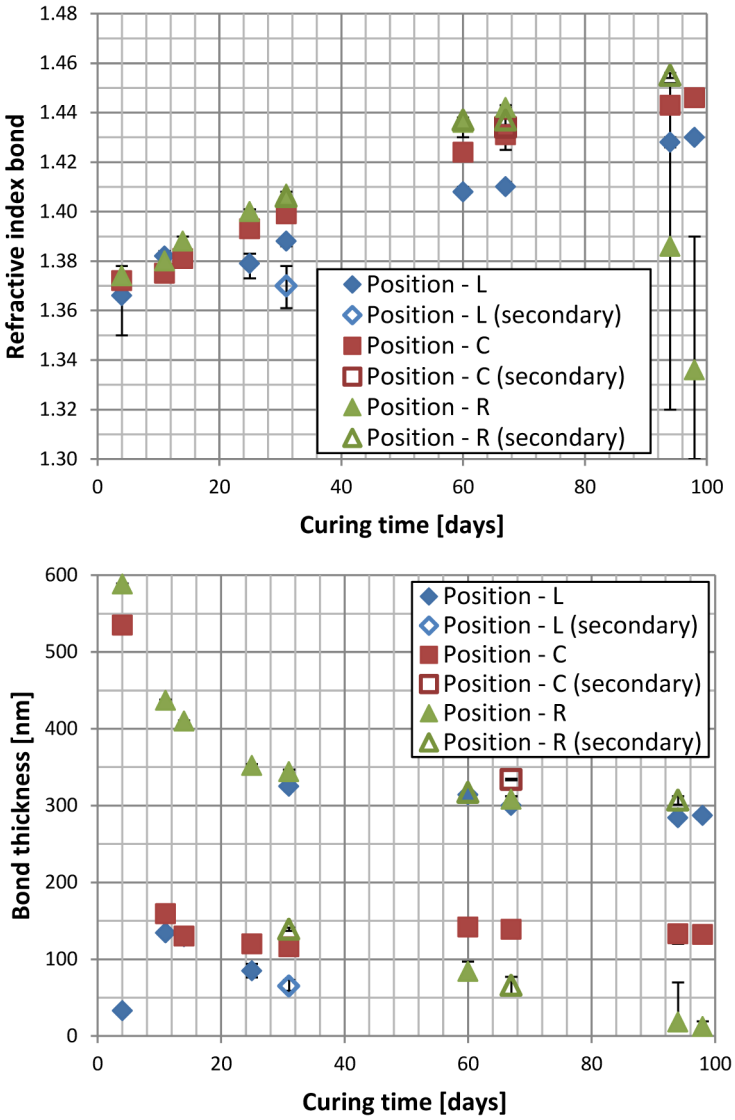

Fig. 9. Top: refractive index of bond as a function of the curing time for the three positions on the front surface. Bottom: thickness of the bond as a function of the curing time for the three positions on the front surface.

The thickness of bond in three different positions does not have as well-defined a trend particularly because the data point with highest probability in some cases swaps between two apparent trend lines. This is particularly noticeable for position 'R'. However, it is possible to infer that bond thickness decreases rapidly (or changes rapidly in location 'L') in the first four weeks and then settles on a constant value (Fig. 9, bottom), different for each position, which can be influenced by the surface figure mismatch of the two bonding surfaces. This is in agreement with the dehydration phase of hydroxide-catalysis bonding: the water, created during the polymerisation, migrates or evaporates in time until a strong and durable bond is formed.

The analysis of flatness maps shows minimum bond thickness ranging from 80 nm in positions 'C' and 'L' to 110 nm in position 'R', whereas the analysis suggests that the thickness after curing ranges between 140 in position 'R' and 300 nm in location 'L' and 'C' suggesting that the bond thickness is in the same order of magnitude as the derived minimum

Optics EXPRESS

bond thickness, but that it is not necessary determined (fully) by the conformity of the substrates bonded together. This is consistent with destructive thickness measurements acquired by slicing and polishing other samples, coating them with a very thin layer of gold and imaging them using atomic force microscopy (AFM) or scanning electron microscopy (SEM) which were polished to nominally 60 nm peak-to-valley. These have previously found thicknesses between 40 and 200 nm. Individual measurements were accurate to ± 20 nm and thickness values varied across the sample [20,24–26].

5. Conclusions

In this paper a powerful and non-destructive technique was outlined for determining the refractive index and thickness of a bond using measurements of optical reflectivity. With Matlab software using Bayesian likelihood analysis and the mathematical model of the reflection of a bond layer between two homogeneous and non-polarising substrates which takes into account thin film interference, the most likely values for bond refractive index and thickness can be extracted from reflectivity data if the refractive index and thickness of the substrate are known.

More specifically, a setup to measure the reflectances of $\perp$ and $\parallel$ linearly polarised incident light of a green laser diode module was realised. The reflectances from the bonded interface between two fused silica discs, jointed using sodium silicate solution, were investigated.

These measurements, together with the realisation of a theoretical model and software based on the Bayesian analysis, have allowed the gain of information not only on the intensity of the light that is reflected from a bonded interface, but also on the refractive index and thickness of the bond in different locations.

It was found that the reflectivity decreased (after initial settling) to less than $1 \cdot 10^{-3}$ at which point limitations to the sensitivity of the setup were reached. This is in agreement with the value obtained by Sinha: he measured reflections from a silicate bond at normal incidence between fused silica parts to be less than $7.08 \cdot 10^{-4}$ [18].

The refractive index was shown to increase with time from 1.36 to 1.45 approaching that of fused silica. This is in line with expected values.

The levels of reflectivity found here are very low, which is what would be required in transmissive parts of e.g. laser gain media which confirms that hydroxide-catalysis bonding is indeed a highly interesting jointing candidate for optical applications. Also, the fact that the refractive index approaches that of the fused silica, explains why the reflectivity becomes so low and it provides scope for tailoring the refractive index of bonds between a variety of materials.

The bond thickness was shown to decrease rapidly in the first four weeks, to then settle down at a constant value. The values found are more ambiguous due to multiple possible solutions for δ_2 (in which d_2 appears; see Eq. (5)). However thickness values are in the same range or slightly larger as the flatness measured for the substrates, which is in line with what has been seen when doing destructive SEM imaging of bonds [20,24–26]. The optical method shown in this paper for determining bond thickness is highly attractive as it is non-destructive. In applications like e.g. the mirror suspensions of interferometric gravitational wave detectors this may allow for in situ non-destructive measurements of the bond thickness which would highly improve the accuracy of the calculation of the thermal noise introduced by the bonds.

The ambiguity of the thickness could be solved by improving the sensitivity of the reflectivity setup further and taking reflectivity measurements at multiple optical wavelengths.

Funding

UK Science and Technology Facilities Council (STFC) (ST/I001085/1, ST/J000361/1, ST/L000946/1), Royal Society (RS) (RG120367, DH120021).

Optics EXPRESS

Acknowledgments

We would like to express our gratitude to the University of Glasgow for the facilities available to allow us to do our research. We are also thankful to our colleagues in the GEO600 and LIGO Scientific Collaboration for their interest in this area. The authors gratefully acknowledge the support of the United States National Science Foundation (NSF) for the construction and operation of the LIGO Laboratory and Advanced LIGO as well as the Science and Technology Facilities Council (STFC) of the United Kingdom, the Max-Planck Society (MPS), and the State of Niedersachsen/Germany for support of the construction of Advanced LIGO and construction and operation of the GEO600 detector. Additional support for Advanced LIGO was provided by the Australian Research Council.